PHYSICAL REVIEW A VOLUME 56, NUMBER 5 NOVEMBER 1997

Multistable localized structures and superlattices in semiconductor optical resonators

D. Michaelis, U. Peschel, and F. Lederer
Friedrich-Schiller-Universität Jena, Max-Wien-Platz 1, D-07743 Jena, Germany
(Received 14 February 1997)

We report on the existence of various periodic transverse patterns and stable localized structures in the optical field of a planar resonator, which exhibits the defocusing saturable nonlinearity of a semiconductor near the band edge. We predict multistability of all feasible patterns as well as of the localized states. Being equal as well as different, stable localized states can organize as clusters or new kinds of periodic patterns (superlattices). The interaction of localized states via their oscillating tails allows the formation of patterns with the same basic units but with different lattice spacing. [S1050-2947(97)50511-7]

PACS number(s): 42.65.Sf, 42.65.Pc

Since the early days of nonlinear optics the optical response of nonlinear planar resonators has attracted much attention. Prominent nonlinear phenomena such as bistability and various kinds of instabilities (modulational instability, Hopf bifurcation) have been predicted theoretically and some of them confirmed experimentally (for an overview see [1–3] and the references therein). Within the past several years spatial or spatiotemporal effects have moved into the center of interest. This concerns in particular the spontaneous formation of different types of patterns and stable localized structures (SLSs). The occurrence of SLSs and organized clusters were predicted in the limit of nascent optical bistability in the vicinity of critical points [4]. Further studies revealed that the formation of SLSs is a more general phenomenon. It could be identified in quasi-one-dimensional resonators for a focusing Kerr nonlinearity in a wide parameter range [5]. Later SLSs were predicted to occur in two-dimensional cavities with saturable focusing [6] or saturable absorptive media [7,8]. To the best of our knowledge no multistability of patterns as well as SLSs could be identified in materials with a defocusing nonlinearity until now. But huge nonlinearities of that kind appear in direct semiconductors at photon energies slightly below the band edge. Evidently, it may be anticipated that effects like pattern and SLS formation can be most easily experimentally verified in those materials. Hence, the aim of this paper is to prove that these effects may occur in this particular environment, that these patterns and SLSs exhibit multistability, and that new kinds of patterns on the basis of SLSs can be generated.

In what follows we restrict ourselves to high-finesse resonators (finesse>10) that exhibit sharp and well-separated Fabry-Pérot resonances. These resonances are characterized by a certain field structure perpendicular to the interfaces of the resonator. Following a well-established procedure (modal or mean-field theory) (see, e.g., [9]) this mode profile can be assumed constant and can thus be separated from the optical field. Hence the field equation that is left describes the transverse dynamics of the mode amplitudes, whereas the profiles only enter that equation via overlap integrals that determine the normalization. The nonlinearly induced refractive index changes are assumed to be proportional to the density N of the excited carriers [10]. Because absorptive losses in the cavity are small compared to the radiative ones the light-induced bleaching of absorption can be dropped in the evolution equation for the transverse optical field u. The driving force of the system is the incident field denoted by u_{in}. The equation of motion for the carrier density N contains effects such as saturation (saturation density N_s), diffusion (diffusion length L_d), and recombination (recombination time T_r). The full set of normalized equations reads as

$$\left[i \frac{\partial}{\partial T} + \frac{\partial^2}{\partial X^2} + \frac{\partial^2}{\partial Y^2} + \Delta + i - N \right] u(X,Y,T) = u_{\mathrm{in}}(X,Y,T), \tag{1a}$$

$$\left[\frac{\partial}{\partial T} + \frac{1}{T_r} - \frac{L_d^2}{T_r} \left(\frac{\partial^2}{\partial X^2} + \frac{\partial^2}{\partial Y^2} \right) \right] N(X,Y,T) = (N_S - N)|u(X,Y,T)|^2, \tag{1b}$$

where X and Y are the transverse coordinates and T denotes the time (for details of the normalization see [9]). To make contact with a typical experimental situation we specify the configuration to be a 0.4876-μm-thick GaAs cavity sandwiched between two Bragg mirrors that consists of 15 (top) and 18 (bottom) pairs of $\lambda/4$ AlAs-GaAs layers, respectively. For an excitation at $\lambda = 897$ nm the characteristic scaling quantities are as follows: length, 1.5 μm; time, 1 ps; incident intensity, 7.5×10^{12} V^2/m^2; carrier density, 1.5×10^{-23} m^{-3}. A recombination time of 1 ns and an ambipolar diffusion constant of 22 cm^2/s result in $T_r \approx 1000$, $L_d \approx 1$. The saturation density 1.5×10^{24} m^{-3} yields the scaled value $N_s = 10$. The scaling depends critically on the specific experimental situation and may vary by more than one order of magnitude. Furthermore we would like to mention that all following considerations hold for vertical cavity surface emitting lasers (VCSELs) operated below the threshold too. In that case the carrier density N in the above equations has to be replaced by its deviation from the stationary value defined by the driving current. In the same sense both the saturation density and the detuning have to be reduced, respectively. Hence the VCSEL offers the additional opportunity to tune the effective value of the saturation density N_s by changing the current.

By solving Eq. (1) in the continuous plane-wave (CPW) limit ($u = u_0$, $N = N_0$, $u_{\mathrm{in}} = u_{\mathrm{in}}^0$) the intensities $|u_0|^2$ and

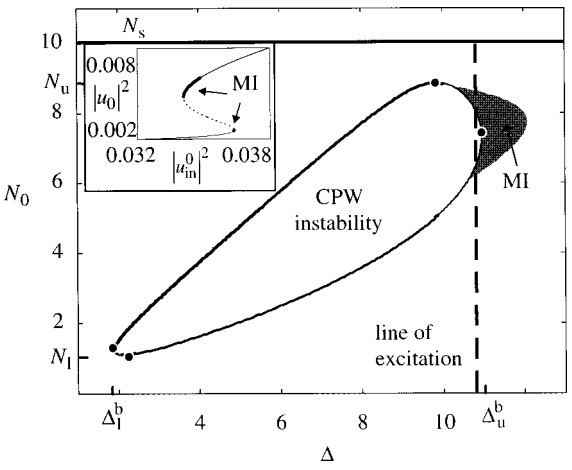

FIG. 1. Domains of CPW stability and instability in the Δ-N_0 plane. The inset shows the hysteresis curve (response curve), which corresponds to an excitation along the dashed line. The dotted line marks the unstable portions; parameters: $T_r=1000$, $L_d=1$, $N_s=10$.

$|u_{\rm in}^0|^2$ can be expressed as functions of the carrier density N_0. A second parameter experimentally accessible is the detuning Δ of the incident beam from the transmission resonance. For a given configuration the CPW solutions are entirely determined by their location in the Δ-N_0 plane. Critical points that mark the onset of instabilities are situated on a closed curve in this plane (see Fig. 1). Unstable solutions are located in the interior of that curve. Concerning the carrier density this curve is bounded by the saturation density N_s. Destabilizations through both limit points and Hopf bifurcations exist. The latter ones only occur for fairly short recombination times compared to the photon lifetime ($T_r<N_s/2-\sqrt{2N_s}$), e.g., in ring resonators. Thus they are not expected to be relevant for the formation of SLSs in the configuration studied here. In what follows we restrict ourselves to parameter domains where no Hopf bifurcation appears.

For a given detuning (fixed experimental situation) the system is restricted to a vertical line in the Δ-N_0 plane (''line of excitation'' in Fig. 1). It corresponds to a hysteresis curve (inset in Fig. 1), which displays the input-output response of the resonator. Multivalued hysteresis loops occur if the ''line of excitation'' crosses regions of CPW instability. The bistable parameter range in the Δ-N plane remains finite due to the saturation of the carrier density. Likewise the nonlinearly induced shift of the resonance is limited, which means that only a certain detuning below a critical value can be compensated. The boundary of the bistable domain is defined as

$$\Delta^b(N_0)=N_0\,\frac{2N_s-N_0}{N_s}\pm\left[\left(N_0\,\frac{N_s-N_0}{N_s}\right)^2-1\right]^{1/2}. \quad (2)$$

Thus, the existence of CPW bistability requires that detuning Δ and carrier density N_0 be bounded between N_u, N_1 and Δ_l^b, Δ_u^b, respectively (see Fig. 1)

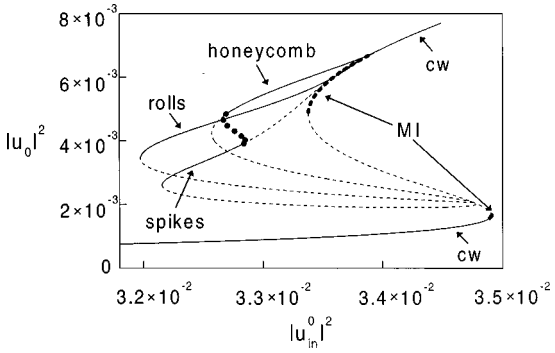

FIG. 2. Hysteresis of different pattern (result of Fourier expansion, dashed lines: unstable). The dots indicate the transition between the two hexagonal patterns; parameters: $T_r=1000$, $L_d=1$, $N_s=10$, $\Delta=10.716$, $k_j^2\approx1$.

$$N_{u,1}=(N_s/2)\left(1\pm\sqrt{1-4/N_s}\right),$$

$$\Delta_u^b=\frac{3}{8}\,N_s[1+2\cos(\Phi/3)],$$

$$\Delta_l^b=\frac{3}{8}\,N_s[1+2\cos(\Phi/3+4\pi/3)], \quad (3)$$

where $\cos\Phi=1-(32/N_s^2)$ and $-\pi\leqslant\Phi\leqslant\pi$.

In the wake of each bistable area in the Δ-N_0 plane a domain of modulational instability (MI) appears. The size of this MI domain is limited by diffusion. An analytical expression for the boundary can be derived straightforwardly.

Another important conclusion can be drawn from Fig. 1. If the excitation is such that the detuning is located near the upper bound of the bistable domain MI may occur above as well as below the limit points (see Fig. 1). This is in contrast to the case without saturation. Consequently, for a fixed input intensity a stable CPW solution can coexist with a modulationally unstable one (see dashed line in Fig. 1). This is a strong indication for the potential existence of at least two types of SLSs, viz., bright SLSs (spikes) on a stable low-transmission and dark SLSs (dips) on a stable high-transmission background.

As it could be anticipated, MI may lead to the formation of stable patterns with the fundamental period related to the modulus of the wave vector of the perturbation where the MI gain is maximum. To analyze how MI develops into patterns we performed a Fourier expansion similar to that in [11], keeping the zeroth- and first-order terms only. Branches of stationary solutions corresponding to different kinds of patterns (rolls, a hexagonal spike pattern, and a honeycomb structure) are displayed in Fig. 2. All stable patterns could be excited numerically by solving the full set of equations (1) with the approximate solution as initial condition and by using periodic boundary conditions (see Fig. 3). Both solutions agree qualitatively.

Some peculiarities are noteworthy. Even if there is no CPW bistability stable patterns may coexist with a CPW background. A similar type of pattern bistability was observed for saturable absorptive media [12]. Moreover a small region can be found where three stable patterns coexist (see Fig. 3). Furthermore a branch that describes the transition

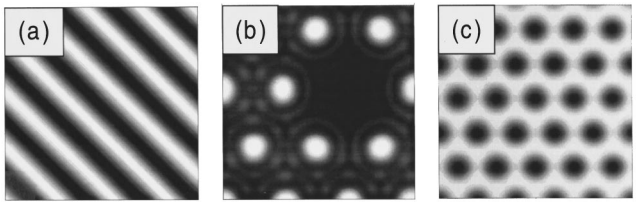

FIG. 3. Multistability of stable patterns: (a) roll pattern, (b) spike pattern with a local defect, (c) honeycomb pattern (carrier concentration). Parameters: same as in Fig. 2 and $|u_{\mathrm{in}}^{0}|^{2}=3.27\times10^{-2}$.

between both hexagon patterns can be identified. Similar effects were found in solving, e.g., the Swift-Hohenberg equation [11]. There the existence of a neutral mode was identified as the relevant physical mechanism. As a matter of fact the zeroth Fourier component of our expansion plays a similar role. But, in contrast to the above case Eq. (1a) contains a genuine quadratic term, i.e., the coupling between field and carrier concentration that also supports the formation of hexagonal patterns.

Different combinations of the CPW solution and a pattern are possible. By a local change of the incident field a localized vacancy can be introduced into the spike pattern, demonstrating the possibility of erasing a single pattern unit [see Fig. 3(b)]. Moreover, even single unit cells of a pattern may exist on a CPW background. To numerically excite these bright SLSs selectively a short excitation pulse is locally added to the background intensity. By matching the beam shape (one- or two-dimensional Gaussian) and diameter to those of the corresponding basic unit of the pattern the particular SLSs are selected. The arising stable SLSs are shown in Fig. 4 and exhibit the common feature of oscillating tails.

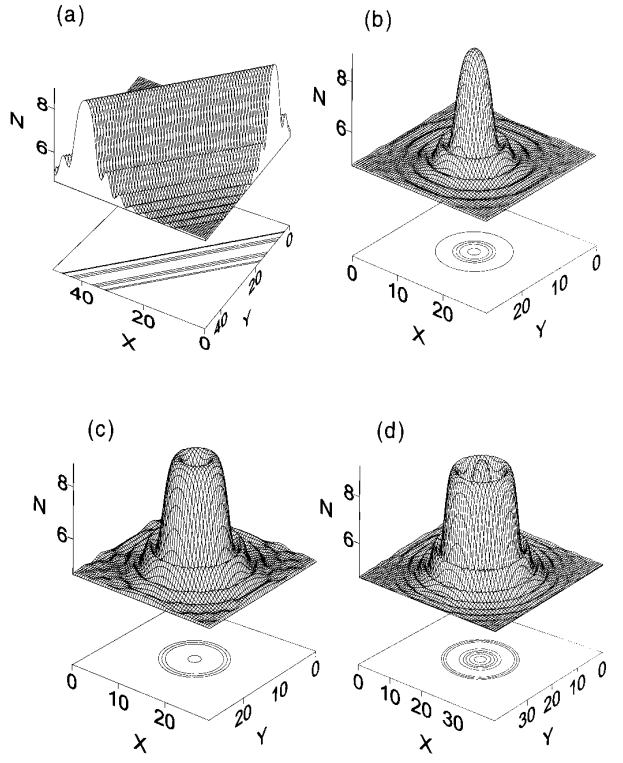

FIG. 4. Multistability of SLSs; same parameters as in Fig. 3.

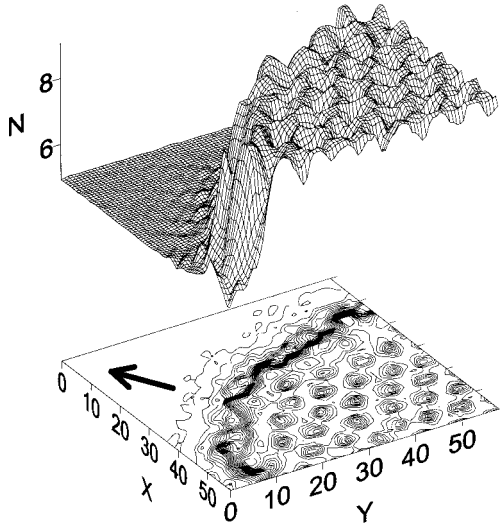

FIG. 5. Hexagonal switching wave; same parameters as in Fig. 3 except $T_r=1$ to minimize the computing effort.

A bright stripe as the basic unit of a roll pattern can be excited by a one-dimensional Gaussian [Fig. 4(a)]. The SLS shown in Fig. 4(b) is a residual of the hexagonal spike pattern. By increasing the beam diameter a stable bright ring develops, which is a basic unit of a honeycomb pattern [Fig. 4(c)]. The diameter of the ring agrees very well with the size of a unit cell of the honeycomb pattern ($d\approx6.2$). If the beam diameter grows larger higher-order filaments with rotational symmetry are excited [Fig. 4(d)]. The excitation of higher-order SLSs by a further increase of the beam diameter becomes progressively difficult. Usually the excited area loses its rotational symmetry due to the onset of MI and emits a hexagonal switching wave (Fig. 5). Here, the transmitted power increases steplike. This nonlinearly induced discreteness is due to the fact that every basic unit of the pattern exhibits a remarkable robustness and switches up like a uniform object. The hexagonal switching wave observed is the discrete counterpart of the homogeneous switching wave found for defocusing Kerr nonlinearities [6,13].

The above examples for SLSs correspond to the situation where the lower branch of the CPW solution is stable and serves as the background. The opposite situation where the high-transmission state is stable and coexists with a SLS may also occur. This can be achieved by decreasing the diffusion length and choosing a detuning where the domain of MI is below the boundary of the bistable domain (see Fig. 6). The resulting dark SLS (stable black holes in a stable high-transmission background) is a residual of a honeycomb pattern and is displayed in the inset of Fig. 6.

After having identified SLSs as residuals of different patterns originating from modulationally unstable CPW solutions we are now going to reverse the procedure. New patterns can be formed with the above SLSs as basic units where two alternative strategies are pursued. The SLSs shown in Fig. 4 represent a coexistence of the CPW background and a basic unit of a particular pattern. The conclusion is now that it might be possible to form a periodic pattern by periodically putting together different SLSs. That this is indeed feasible is shown in Fig. 7(a) where one bright stripe [Fig. 4(a)] and rings [Fig. 4(c)] are combined. They form a new periodic pattern but with an increased unit cell.

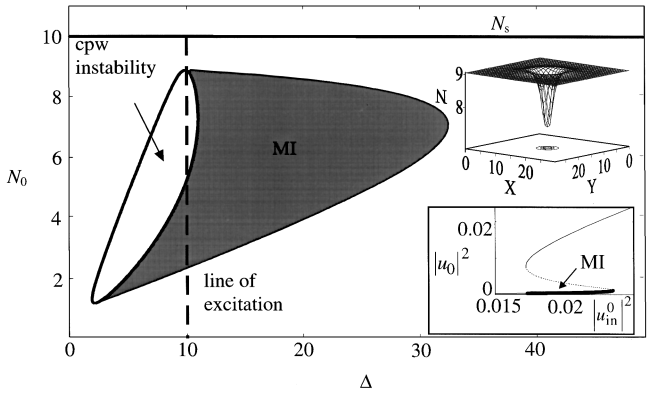

FIG. 6. Dark localized states. Shown are the domains of CPW stability and instability in the Δ-N_0 plane. The insets display the SLS (top) as well as the hysteresis curve (bottom), which corresponds to an excitation along the dashed line in the Δ-N_0 plane (dashed line unstable; parameters: $T_r=1000$, $L_d=0.15$, $N_s=10$. $|u_{\mathrm{in}}^0|^2=1.81\times10^{-2}$, $\Delta=10$).

Thus, the constraints concerning the size of the unit cell are lifted and lattices with different properties may be anticipated. The alternative in forming new patterns consists in changing the spacing between the individual SLSs, which eventually constitute the pattern. All SLSs shown in Fig. 4 exhibit oscillating tails. As already known from quite different nonlinear evolution equations [14] SLSs with oscillating tails may form bound states where the spacing attains discrete values. A hexagonal pattern that is composed of SLSs shown in Fig. 4(c) (rings with central spikes) is plotted in Fig. 7(b). It exhibits features of both hexagonal patterns displayed in Fig. 3 because a low transmission background coexists with residuals of the honeycomb pattern. In contrast to the honeycomb the SLSs forming the pattern are bound by their oscillating tails.

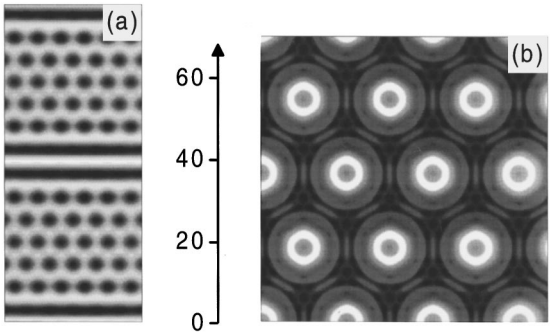

FIG. 7. New kinds of patterns: (a) superlattice formed by honeycomb and rolls; (b) ringlike spike pattern bounded by oscillating tails, same parameters as in Fig. 4.

In conclusion, we have studied the optical response of a resonator filled with a defocusing saturable material. First we identified various types of patterns that coexist with a stable CPW background and show multistability for certain parameters. Various SLSs can survive as residuals of these patterns. All SLSs on a low-transmission background may coexist in a certain parameter range, which represents some kind of multistability of SLSs and patterns. This multistability of SLSs might be of some interest for practical implementations as, e.g., the coding of different signal levels at one site of an all-optical processor.

Different SLSs can be combined to form new patterns, which may be considered as superlattices. The interaction of SLSs via their oscillating tails allows the formation of patterns with the same basic units but with different lattice spacing.

The research was carried out in the framework of the Sonderforschungsbereich 196, Deutsche Forschungsgemeinschaft, Bonn.

[1] N. B. Abraham and W. J. Firth, J. Opt. Soc. Am. B **7**, 951 (1990).
[2] L. A. Lugiato, in *Chaos, Solitons & Fractals* (Pergamon Press, New York, 1994), Vol. 4, pp. 1251–1258.
[3] L. A. Lugiato, Wang Kaige, and N. B. Abraham, Phys. Rev. A **49**, 2049 (1994).
[4] M. Tlidi, P. Mandel, and R. Lefever, Phys. Rev. Lett. **73**, 640 (1994).
[5] Moloney and H. M. Gibbs, Phys. Rev. Lett. **58**, 2209 (1987).
[6] N. N. Rosanov and G. V. Khodova, J. Opt. Soc. Am. B **7**, 1057 (1990).
[7] W. J. Firth and A. J. Scroggie, Phys. Rev. Lett. **76**, 1623 (1996).
[8] M. Brambilla, L. A. Lugiato, and M. Stefani, Europhys. Lett. **34**, 109 (1996).
[9] F. Lederer, T. Peschel, and U. Peschel, Pure Appl. Opt. **2**, 635 (1993).
[10] N. Finlayson, E. M. Wright, and G. I. Stegeman, IEEE J. Quantum Electron. **26**, 770 (1990).
[11] C. B. Price, Phys. Lett. A **194**, 385 (1994).
[12] W. J. Firth and A. J. Scroggie, Europhys. Lett. **26**, 521 (1994).
[13] W. J. Firth, I. Galbraight, and E. M. Wright, J. Opt. Soc. Am. B **12**, 1005 (1995).
[14] B. A. Malomed, Phys. Rev. E **47**, 2874 (1993).